Modeling the Particle Size and Interfacial Hardening Effects in Metal Matrix Composites with Dispersed Particles at Decreasing Microstructural Length Scales

Rashid K. Abu Al-Rub[*]

Aerospace and Mechanical Engineering, University of Notre Dame, Notre Dame, IN 46556, USA

ABSTRACT

The focus of this paper is on incorporating the particle size effect and the effect of particle-matrix interfacial properties on the average onset of plasticity and strain hardening rates of metal matrix composites reinforced with hard, stiff, or soft particles. In order to achieve this objective, a higher-order gradient plasticity theory that explicitly includes the effect of interfacial energy at particle-matrix interfaces is formulated within the frameworks of virtual power and thermodynamic laws. The derived higher-order gradient plasticity theory also takes into account large variations in plastic strain tensor and effective plastic strain; namely, the gradient of plastic strain, the gradient of the effective plastic strain, and the accumulation of plastic strain gradients. Moreover, unlike the majority of the existing gradient plasticity theories in the literature, it is shown that the matrix nonlocal yield condition as well as a yield-like condition for the particle-matrix interface can be directly derived from the principle of virtual power without any further constitutive assumptions. Also, in this work the interfaces dissipate energy similar to the bulk material during plastic deformation. The interfacial yield condition takes into consideration the particle type (soft, stiff, hard) through the incorporation of the particle-matrix interfacial yield strength and interfacial hardening in case of dislocation transmission across the interface (i.e. shearing of particles). The proposed higher-order gradient plasticity theory is shown to be qualitatively successful in predicting the increase in the average yield strength, strain hardening rates, and flow stress as the particle size decreases and the particle interfacial strength increases.

KEYWORDS

interfacial yield strength, interfacial hardening, particles (inclusions), gradient plasticity, nonlocal, size effect

*Address all correspondence to rabualrub@civil.tamu.edu.

1. INTRODUCTION

Advanced metal matrix composites (AMMCs; i.e., pure metals or metallic alloys with dispersed particles or inclusions at decreasing microstructural length scales ranging in size from a few micrometers down to hundreds of nanometers) with mechanical and physical properties well in excess of those exhibited by conventional metal matrix composites (i.e., pure metals or metallic alloys that consist of large particles, fibers, whiskers, etc.) are of considerable economic, technological, and scientific interest and will contribute significantly to the heightened performance of structural components and systems in many industries. For example, with the introduction of stronger safety legislation and increased fuel prices, auto manufacturers are striving for increasing the car body stiffness for safety and lowering the body weight for fuel efficiency by designing a new generation of advanced high-strength steels (AHSS) embedded with metallic and/or ceramic particles of different sizes. Figure 1 shows an AHSS embedded with inclusions at two distinct scales: Primary particles (such as titanium nitrides) are typically on the order of several microns in size, and secondary particles (such as titanium carbides and manganese sulfides) are on the order of hundreds of nanometers in size.

Generally, second-phase particles play a dual role: (1) On one hand, depending on their size and interfacial hardening properties, they can significantly increase the strength and improve the plastic work-hardening behavior; (2) on the other hand, depending on their strength and interfacial strength, particle cracking and/or interfacial debonding cause nucleation, growth, and coalescence of microvoids and microcracks, which eventually lead to damage induced-anisotropy and ductile failure. Many researchers have investigated the interfacial damage effects (e.g., [1–14]), whereas very few have researched the interfacial strengthening and hardening mechanisms due to varying particle sizes and varying particle-matrix interfacial properties. Therefore the focus of this article is on the particle size and interfacial hardening effects in AMMCs. Several experimental works on particle-reinforced composites have revealed that a substantial increase in the macroscopic yield strength and flow stress can be achieved by decreasing the particle size, while keeping the volume fraction constant (e.g., [15–20]). Therefore there is great need for the development of a mechanical theory that can accommodate size effects in AMMCs and that can be used for bridging the length scales.

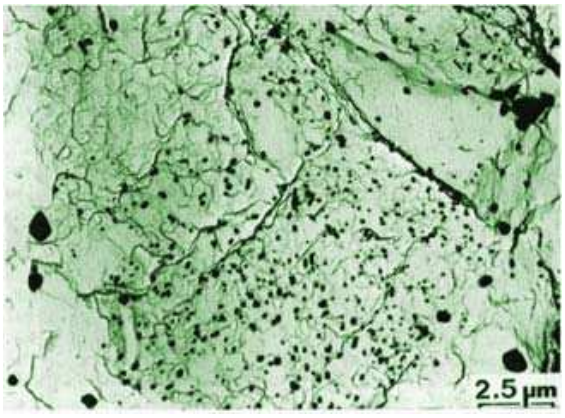

FIGURE 1. A transmission electron microscopy (TEM) micrograph of the microstructure of an ultra-high-strength steel showing the different levels of dispersed small particles

Theoretical modeling and multiscale computational simulations are necessary for the design of new generations of AMMCs. Therefore it is imperative to develop a constitutive model and a multiscale framework that can be used successfully in incorporating the strengthening effects due to the reduction in particle (inclusion) size and the effects of the interfacial hardening by incorporating the particle-matrix interfacial mechanical properties (e.g., interfacial strength and hardening). Unfortunately, the classical continuum plasticity theories (e.g., von Mises or Drucker-Prager) are unable to predict the influence of particle size due to the absence of a microstructural length scale parameter in their constitutive equations (e.g., [5, 21–24]). Therefore, within a classical continuum mechanics framework, the mechanical properties of multiphase materials only depend on the volume fraction of particles, while the particle size is not accounted for. However, the mechanical properties of advanced materials, with a typical distance D between particles and particle size d, depend on how these geometrical parameters interfere with other characteristic distances such as the mean-free path of dislocations. Reducing the size of particles, while keeping the volume fraction constant, significantly improves the material macroscopic mechanical prop-

erties. Furthermore, there are several other types of size effects that the classical continuum theories fail to predict. For example, experimental works have shown an increase in strength by decreasing (1) the diameter of microwires under torsion [23], (2) the thickness of thin films under bending or uniaxial tension (e.g., 25–30]), (3) the indentation depth in micro/nano indentation tests (e.g., 31–38]), (4) the grain size of nanocrystalline materials (the well-known Hall-Petch effect), (5) the void size in nanoporous media, and several others.

Since the increase in strength with decreasing scale can be related to a proportional increase in the strain gradients in each of the aforementioned experiments, the gradient plasticity theory has been successful in addressing the size effect problem. This success stems from the incorporation of a microstructural length-scale parameter through functional dependencies on the plastic strain gradient of nonlocal media [39, 40]. The gradient-dependent theory abandons the assumption that the stress at a given point is uniquely determined by the history of strain at this point only. It takes into account possible interactions with other material points in the vicinity of that point. However, in the past decade, the physical basis of the gradient plasticity theory for metals has been founded on theoretical developments concerning geometrically necessary dislocations (GNDs) [41]. Standard micromechanical modeling of the inelastic material behavior of metallic single crystals and polycrystals is commonly based on the premise that resistance to glide is due mainly to the random trapping of mobile dislocations during locally homogeneous deformation. Such trapped dislocations are commonly referred to as statistically stored dislocations and act as obstacles to further dislocation motion, resulting in hardening. As anticipated in the work of Ashby [21], an additional contribution to the density of immobile dislocations, and so to hardening, can arise when the continuum length scale approaches that of the dominant microstructural features. An extensive review of the recent developments in gradient-dependent theory can be found in Voyiadjis and Abu Al-Rub [42]. A short review of these developments is presented here.

Many researchers have contributed substantially to the gradient approach, with emphasis on numerical aspects of the theory and its implementation in finite element codes (e.g., [43–52]). In parallel, other approaches that have length-scale parameters in their constitutive structure (commonly referred to as nonlocal integral theories) have appeared as an outgrowth of earlier work by Eringen in nonlocal continuum elasticity and phenomenological hardening plasticity (e.g., [53]) and Bazant in strain softening media (e.g., [54, 55]). Another class of gradient theories has been advocated in the last two decades that assume higher-order gradients of the plastic strain field (e.g., [56–71]). This group of theories is in fact a particular case of the generalized continua, such as *micromorphic continua* [72] or *continua with microstructure* [73], which were all inspired by the pioneering work of the Cosserat brothers [74]. The *Cosserat continuum* (or *micropolar continuum*) enhances the kinematic description of deformation by an additional field of local rotations, which can depend on the rotations corresponding to the displacement field, that is, on the skew-symmetric part of the displacement gradient for the small-displacement theory or on the rotational part of the polar decomposition in the large-displacement theory. However, the works of Mindlin, Cosserat, and Eringen are based on the classical balances of linear and angular momentum. In contrast, the works of Fleck, Gurtin, Gudmundson, and Abu Al-Rub involve the introduction of additional balances over and above these classical balances; for example, for single-crystal plasticity, there is a new balance for each slip system involving forces that expend power in consort with slip on that system. Moreover, dislocation-based gradient plasticity theories that are motivated by the generation of GNDs and incompatibility of lattice deformation have been advanced [75–81]. However, these theories preserve the same structure of classical plasticity, with no explicit accounting for the microscopic additional boundary conditions that should be enforced at free surfaces and constrained interfaces.

Numerous variational formulations and thermodynamic frameworks have also been proposed since the 1990s to extend the classical (local) constitutive theory to a nonlocal (gradient-dependent) theory. However, these constitutive models are far from being firmly established. Moreover, the various proposals are also quite different with respect to the structure of the equations. Mühlhaus and Aifantis [82] formulated the classical (local) incremental variational principle by incorporating first-

order gradients of the effective (scalar) plastic strain variable, which contributes to the isotropic hardening/softening plasticity. Extra boundary conditions and higher-order stresses were derived. However, in their formulation, the higher-order tractions that result from higher-order gradients were not considered. Fleck and Hutchinson [59] reformulated their earlier theory [57, 58] based on the variational principle of [82], but with different constitutive structure. In the formulation of [59], higher-order tractions, higher-order stresses, and extra boundary conditions were derived. Valanis [83] and Fremond and Nedjar [84] postulated the dependence of the Helmholtz free energy on scalar variables and on its first-order gradients. Additionally, they checked the consistency of their constitutive equations using the classical (local) form of the Clausius-Duhem inequality. However, Polizzotto (e.g., [85, 86]) assumed a nonlocal form of the Clausius-Duhem inequality based on the concept of the nonlocality energy residual introduced by [53]. First- and second-order gradients of the effective plastic strain were incorporated in their formulation, in which the nonlocality residual enters the definition of the Clausius-Duhem inequality as an extra term that accounts for the energy exchanges between the particles in the domain of interest at the microstructural level. Moreover, Polizzotto proposed the insulation condition, which assumes the vanishing of the total nonlocal residuals over the whole volume of the body, to derive the extra boundary conditions. The thermodynamic framework of Polizzotto was used by Steinmann (e.g., [87, 88]) to derive several strain gradient plasticity models into which the second-order gradient of the effective plastic strain was incorporated. Shizawa and Zbib [89] derived a rigorous thermodynamical theory of finite strain gradient plasticity by incorporating kinematic gradient hardening effects through the concept of a dislocation density tensor. A similar gradient-based thermodynamic framework was proposed by [90]. Another thermodynamic approach was developed by Gurtin (e.g., [64–67]), who treated the plastic strain gradients as independent variables, differently from the above frameworks, and introduced the concept of microforce balance, which is shown in [70] to be equivalent to the nonlocal yield condition. Gurtin introduced both isotropic (dissipative) and kinematic (energetic) gradient hardening effects and argued that the plastic flow direction is governed by a microstress, obtained from the microforce balance, and not the deviatoric Cauchy stress. In Gurtin's framework, however, only the kinematic (energetic) hardening variables enter the variational formulation, without the isotropic hardening variables. Isotropic hardening is incorporated through constitutive assumptions that postulate the additive decomposition of the higher-order gradient conjugate force into an energetic part and a dissipative part. A very similar variational and thermodynamical framework has been proposed by [69]. Bammann [78] has developed a very attractive dislocation-based thermodynamic framework that incorporates the effect of geometrically necessary dislocations through the curl of the plastic deformation gradient. Thermodynamic approaches to gradient-dependent plasticity and damage models were developed by Voyiadjis et al. [91, 92] and Abu Al-Rub and Voyiadjis [80, 81], who postulated the dependence of the Helmholtz free energy on scalar and tensorial hardening/softening variables and its second-order gradients. However, no explicit treatment of nonstandard boundary conditions was considered in this framework. Clayton et al. [79] presented a novel finite deformation thermodynamic framework to describe spatial rotational gradients in crystals by introducing a mathematical concept for geometrically necessary disclinations at grain boundaries. However, the effects of these rotational gradients are expected to be minimal in small-strain problems.

The gradient theory has been applied to interpret size-dependent phenomena, including shear banding, micro- and nanoindentation, twist of thin wires, bending of thin films, void growth, crack tip plasticity, fine-grained metals, strengthening in metal matrix composites, multilayers, and so on (see [42] for a detailed review). Therefore practical applications of gradient-dependent theories include, but are not limited to, sensors, actuators, microelecromechanical systems, microelectronic packaging, advanced composites, micromachining, welds, and functionally graded materials. However, the full utility of the gradient-type theories in bridging the gap between modeling, simulation, and design of modern technology hinges on one's ability to determine accurate values for the constitutive length-scale parameter that scales the effects of strain gradients. This issue has been peripherally addressed by [60, 93–95]. A more rigorous identification of the

material length scale from microdeformation experiments and its physical interpretation based on dislocation mechanics has been presented by [80, 96–99]. Abu Al-Rub and Voyiadjis [96] have shown that indentation experiments are the most effective test for measuring the length scale parameter ℓ in the gradient plasticity theory. Moreover, they have shown that this material length scale is proportional to the average spacing between dislocations (or the dislocation mean free path or the dislocation cell size) such that it cannot be assumed constant or fixed, but instead evolves with the course of plastic deformation and microstructural features (e.g., grain size, inclusion size). Abu Al-Rub and Voyiadjis [97] also derived an evolution equation for ℓ as a function of temperature, strain, strain rate, and a set of measurable microstructural physical parameters. Voyiadjis and Abu Al-Rub [99] and Abu Al-Rub and Voyiadjis [80, 81] found that the length scale varies with the course of plastic deformation, grain size, characteristic dimension of the specimen, and strain-hardening exponent.

However, of the aforementioned gradient plasticity theories, very few have emphasized the physical nature of the additional (nonclassical) boundary conditions that result from the mathematical treatment of gradient plasticity within the variational framework. Starting from the work of Gudmundson [69], Aifantis and Willis [24, 100], Fredriksson and Gudmundson [101], and Abu Al-Rub et al. [70] have shown that these additional microscopic boundary conditions can be expressed physically in terms of the surface or interfacial energy at free surfaces and interfaces of micro/nano structured metals. Recently, Abu Al-Rub [102] investigated different mathematical forms of the interfacial energy and formulated, besides the yield condition for the bulk, a yieldlike condition at the interface. Therefore the introduction of interfacial energies at the particle-matrix interfaces in advanced metallic composites allows one to incorporate the interfacial mechanical properties of interfaces (e.g., interfacial yield strength and hardening) such that dislocation emission and transmission at interfaces can be accounted for explicitly. Therefore different stiffnesses of the particle-matrix interface can be considered (e.g., hard, stiff, intermediate, and soft), depending on the level of interfacial energy.

The objective of this article is to extend and utilize the preceding frameworks of gradient plasticity to address the problem of strain hardening in particle-reinforced metal matrix composites due to particle or inclusion size effects. The pioneering works contributed by, among others, Aifantis, Eringen, Gurtin, Polizzotto, Fleck, and Hutchinson, and their coworkers, have been a source of inspiration for this work. Therefore a unified treatment of gradient plasticity to address size hardening effects in advanced composites is presented in this article. Emphasis is placed on bulk and interfacial hardening effects, whereas bulk and interfacial softening effects (e.g., particle debonding) will be presented in a future work. Moreover, since the works of Abu Al-Rub et al. [70] and Abu Al-Rub [102] assume nondissipative interfaces, the internal virtual and thermodynamic frameworks of Abu Al-Rub et al. [70] for strain gradient plasticity theory are modified here to include interfacial dissipation effects such that besides the dissipation energy within the bulk or the matrix, the interface is allowed to dissipate energy due to interfacial plastic deformation. Furthermore, an additional internal state variable is introduced in the formulation of Abu Al-Rub et al. [70] for the sake of completeness in describing the large variations in plastic strains at small length scales. Thus, besides the gradient of plastic strain tensor and the gradient of effective (equivalent or accumulative) plastic strain, the accumulation of the plastic strain gradients is also incorporated as an additional internal state variable, which leads to additional hardening effects. Furthermore, the recent study by Abu Al-Rub [102] is used to guide the proper mathematical form for the interfacial energy function at the particle-matrix interface.

The layout of the article is as follows: In Section 2, the nonlocal plasticity theory is formulated based on the principle of virtual power and laws of thermodynamics. The bulk (matrix) and interface (particle-matrix interface) gradient hardening effects are considered in a unified framework. In Section 3, the physical interpretations of the two material length scales, one for the bulk and another for the interface, are presented. In Section 4, an application of the formulated theory for predicting the size-scale effects in particle-reinforced metal matrix composites is presented.

Hereafter, $||\ ||$ is the Euclidean norm of second rank tensors, $(:)$ stands for tensor contraction, the superimposed dot $(\cdot)$ indicates the differentiation with respect to time t, and a comma fol-

lowed by an index i denotes differentiation with respect to x_i. The first-order gradient, divergence, curl, and Laplacian of a second-order tensor field A are defined by $(\nabla A)_{ijk} = A_{ij,k}$, $(\mathrm{div}\, A)_i = A_{ij,j}$, $(\mathrm{curl}\, A)_{ij} = e_{ipq}A_{jq,p}$, and $(\nabla^2 A)_{ij} = A_{ij,kk}$, respectively.

2. NONLOCAL THERMODYNAMIC FORMULATION

The formulation of a continuum-based plasticity model requires the satisfaction of the axioms of equilibrium and thermodynamics. This section presents the principle of virtual power and the fundamental statements of irreversible thermodynamics that are commonly used in the mathematical modeling of the material thermomechanical behavior.

2.1 Basic Kinematics and Assumptions

The classical theory of isotropic plastic solids undergoing small deformations is based on the additive decomposition of the total strain rate into elastic and plastic parts, where $\boldsymbol{\varepsilon}^e$ is the elastic component and $\boldsymbol{\varepsilon}^p$ is the corresponding plastic component such that

$$\dot{\varepsilon}_{ij} = \dot{\varepsilon}^e_{ij} + \dot{\varepsilon}^p_{ij}, \quad \dot{\varepsilon}^p_{kk} = 0 \tag{1}$$

where the superscripts e and p designate the elastic and plastic components, respectively. The second-order tensor, $\dot{\boldsymbol{\varepsilon}}$, is the rate of deformation, which is defined by the symmetric part of the velocity gradient $v_{i,j}$:

$$\dot{\varepsilon}_{ij} = \frac{1}{2}\left(v_{i,j} + v_{j,i}\right) \tag{2}$$

In classical continuum plasticity, the isotropic hardening variable (history variable), $\dot{p}$, is defined as the rate of the local effective plastic strain and is expressed by

$$\dot{p} = \left\|\dot{\varepsilon}^p_{ij}\right\| = \sqrt{\dot{\varepsilon}^p_{ij}\dot{\varepsilon}^p_{ij}} \tag{3}$$

Moreover, one can define the unit direction of the plastic strain as

$$N_{ij} = \frac{\dot{\varepsilon}^p_{ij}}{\left\|\dot{\varepsilon}^p_{ij}\right\|} = \frac{\dot{\varepsilon}^p_{ij}}{\dot{p}} \tag{4}$$

such that one can write

$$\begin{aligned} \|N_{ij}\| = N_{ij}N_{ij} = 1 \quad &\Rightarrow N_{ij}\frac{\dot{\varepsilon}^p_{ij}}{\dot{p}} = 1 \\ \Rightarrow N_{ij}\dot{\varepsilon}^p_{ij} = \dot{p} \quad &\Rightarrow \quad \dot{\varepsilon}^p_{ij} = \dot{p}N_{ij} \end{aligned} \tag{5}$$

where the last expression in the above equation corresponds to the flow rule definition in the classical plasticity theory. Operating on the rate of effective plastic strain in Eq. (3) by the first-order gradient yields

$$\dot{p}_{,k} = \frac{\dot{\varepsilon}^p_{ij}\dot{\varepsilon}^p_{ij,k}}{\sqrt{\dot{\varepsilon}^p_{mn}\dot{\varepsilon}^p_{mn}}} = \frac{\dot{\varepsilon}^p_{ij}}{\dot{p}}\dot{\varepsilon}^p_{ij,k} = N_{ij}\dot{\varepsilon}^p_{ij,k} \tag{6}$$

a useful result that will be used in subsequent developments.

Now, to be able to model the effect of the particle size on the strength of AMMCs, higher-order plastic strain gradients should be incorporated into the formulation of a plasticity theory. This can be done by assuming that the internal energy depends not only on the internal state variables $\boldsymbol{\varepsilon}^p$ and p, as in the classical plasticity theory, but also on its spatial higher-order gradients $\nabla\boldsymbol{\varepsilon}^p$ and ∇p. The third-order tensor $(\nabla\boldsymbol{\varepsilon}^p)_{ijk} = \varepsilon^p_{ij,k}$ introduces anisotropy through kinematic hardening, which is attributed to the net Burgers vector being not equal to zero at the microscale [103]. The first-order gradient $(\nabla p)_k = p_{,k}$ introduces isotropic hardening or internal history, which is attributed to the accumulation of the so-called GNDs [21]. Indeed, for metal matrix micro/nano composites, the resulting deformation incompatibility between, for example, hard or soft inclusions, due to elastic modulus and coefficient of thermal expansion mismatch, is accommodated by the development of GNDs (see Fig. 2). The plastic strain gradient, $\nabla\boldsymbol{\varepsilon}^p$, is related to the GND density tensor, $\boldsymbol{G}$, through the following relation [41, 103]:

$$G_{ij} = e_{irq}\varepsilon^p_{jq,r} \tag{7}$$

where e_{irq} is the permutation symbol. In addition, the gradient of the effective plastic strain, ∇p, is related to the effective density of GND, ρ_G, through the following relation [21]:

$$\rho_G = \frac{1}{b}\sqrt{p_{,k}p_{,k}} \tag{8}$$

where b is the magnitude of the Burgers vector. Therefore the presence of higher-order gradients

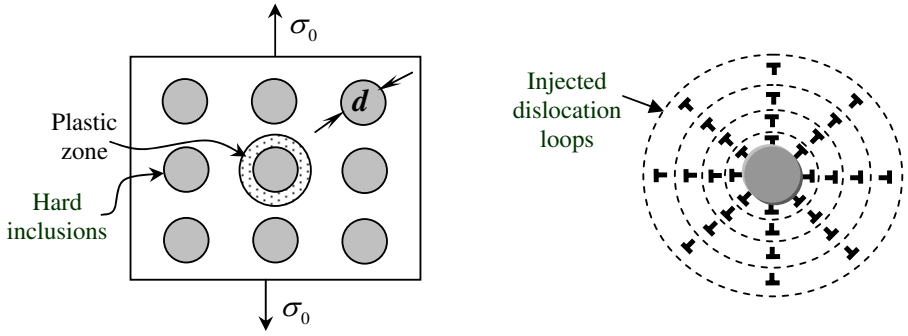

FIGURE 2. Plastic strain gradients are caused by evolution of geometrically necessary dislocations around spherical inclusions of size d under uniaxial loading

through the plastic strain tensor (i.e., $\nabla\boldsymbol{\varepsilon}^p$) leads to higher-order gradients in the accumulation of plastic strain (i.e., ∇p) such that one cannot exist without the other. Furthermore, because of the presence of both $\nabla\boldsymbol{\varepsilon}^p$ and ∇p, the total rate of accumulation of the plastic strain gradients,

$$\dot{e} = \sqrt{\dot{\varepsilon}^p_{ij,k}\dot{\varepsilon}^p_{ij,k}} = \sqrt{\dot{p}_{,k}\dot{p}_{,k}} \quad \text{with} \quad e = \int_0^t \dot{e}\, dt \tag{9}$$

should also be considered in the constitutive description as it introduces additional isotropic hardening [71]. Note that Eq. (6) is used for obtaining Eq. (9) and assumes that $\nabla\boldsymbol{N} = 0$, which implies that if yielding occurs at a material point, then the surrounding volume of a deformation zone of diameter ℓ has also yielded (i.e., plastic localization zone) and that there is no change in the plastic flow direction within ℓ.

Similar to the definition of direction of the plastic strain, $\boldsymbol{N}$, defined in Eq. (4), one can define the directions of the plastic strain gradient, $\nabla\boldsymbol{\varepsilon}^p$, and the gradient of the effective plastic strain, ∇p, respectively, as

$$\begin{aligned} M_{ijk} &= \frac{\dot{\varepsilon}^p_{ij,k}}{\left\|\dot{\varepsilon}^p_{ij,k}\right\|} = \frac{\dot{\varepsilon}^p_{ij,k}}{\dot{e}} \Rightarrow \dot{\varepsilon}^p_{ij,k} = \dot{e}\, M_{ijk} \\ \mathrm{N}_k &= \frac{\dot{p}_{,k}}{\|\dot{p}_{,k}\|} = \frac{\dot{p}_{,k}}{\dot{e}} \Rightarrow \dot{p}_{,k} = \dot{e}\, \mathrm{N}_k \end{aligned} \tag{10}$$

where $\boldsymbol{M}$ and $\mathbf{N}$ define the unite tensors of $\nabla\boldsymbol{\varepsilon}^p$ and ∇p, respectively, such that $\boldsymbol{M} : \boldsymbol{M} = \mathbf{N} : \mathbf{N} = 1$. Therefore one can easily show from Eqs. (10) and (6) that $\boldsymbol{N}$, $\boldsymbol{M}$, and $\mathbf{N}$ are related by the following identity:

$$N_{ij} M_{ijk} \mathrm{N}_k = 1 \tag{11}$$

Moreover, from Eqs. (4), (10), and (6), one can easily write

$$\dot{p} = \dot{\varepsilon}^p_{ij} N_{ij}, \quad \dot{p}_{,k} = \dot{\varepsilon}^p_{ij,k} N_{ij}, \quad \dot{e} = \dot{\varepsilon}^p_{ij,k} M_{ijk} \tag{12}$$

Utilizing Eq. (11), one can write the right-hand Eq. (12) as

$$\dot{e} = \dot{\varepsilon}^p_{ij,k} N_{ij} \mathrm{N}_k \tag{13}$$

Therefore the generalized rate of total accumulation of the plastic strain and plastic strain gradients can be defined as

$$\begin{aligned} \dot{E}^2 &= \dot{p}^2 + \ell^2 \dot{e}^2 = \dot{p}^2 + \ell^2 \dot{p}_{,k}\dot{p}_{,k} \\ &= \dot{\varepsilon}^p_{ij}\dot{\varepsilon}^p_{ij} + \ell^2 \dot{\varepsilon}^p_{ij,k}\dot{\varepsilon}^p_{ij,k} \end{aligned} \tag{14}$$

where ℓ is the material length scale parameter used for dimensional consistency and $E = \int_0^t \dot{E}\, dt$ is the nonlocal effective plastic strain, which is intended to measure the total dislocation density. With the absence of plastic strain gradients, E reduces to the local effective plastic strain p. Hence, for a complete nonlocal constitutive description at small length scales, the internal power and the Helmholtz free energy should include not only the effects of $\boldsymbol{\varepsilon}^p$ and p, but also the effects of $\nabla\boldsymbol{\varepsilon}^p$, ∇p, and e. Analogous to the history variable in classical plasticity theory, p, the nonlocal history variable, e, introduces the history in the accumulation of $\nabla\boldsymbol{\varepsilon}^p$ and ∇p. Furthermore, although $\boldsymbol{\varepsilon}^p$, p, $\nabla\boldsymbol{\varepsilon}^p$, ∇p, and e may have a common origin in dislocation storage

and motion, they will be treated independently of each other. This gives different physical interpretations that guide one to different evolution equations and allow one to computationally introduce the influence of one scale on the other (e.g., the effect of mesoscale on macroscale). However, those variables are considered here as mathematically related to their local counterparts, and therefore special care must be taken to properly account for their coupling.

Moreover, some authors have considered in their thermodynamics formulations only the gradient of the plastic strain $\nabla\boldsymbol{\varepsilon}^p$, whereas others have considered only the gradient of the effective plastic strain ∇p, and others have considered the effect of both $\nabla\boldsymbol{\varepsilon}^p$ and ∇p. For example, Fleck and Hutchinson [59], Gao et al. [61], Gurtin [66, 67], and Gudmundson [69] have developed gradient theories that allow dependences on $\nabla\boldsymbol{\varepsilon}^p$ only. However, the theories of Fleck and Hutchinson [59] and Gao et al. [61] introduce $\nabla\boldsymbol{\varepsilon}^p$ such that only the isotropic hardening is included, without kinematic hardening (i.e., no Bauschinger effect). Gurtin [66, 67] did not incorporate ∇p in his variational formulation (i.e., the internal virtual power) but incorporated it in the functional definition of the Helmholtz free energy. Aifantis [39], Mühlhaus and Aifantis [82], Acharya and Bassani [75], Liebe and Steinmann [88], and Polizzotto and Borino [85] have developed gradient theories that allow dependences on ∇p. Voyiadjis et al. [91, 92, 104] introduced first- and second-order gradients in both isotropic and kinematic hardening. However, the kinematic hardening was introduced through an arbitrary flux variable. Recently, Abu Al-Rub et al. [70], Abu Al-Rub [102], and Voyiadjis and Abu Al-Rub [71] have included the effect of both $\nabla\boldsymbol{\varepsilon}^p$ and ∇p in the definitions of the internal virtual power and the Helmholtz free energy. In the following, the dependence of the internal virtual power and Helmholtz free energy on $\nabla\boldsymbol{\varepsilon}^p$, ∇p, and e is the essential ingredient of the present strain gradient plasticity to incorporate size effects. It is argued that none of these variables exist without the other such that in formulating a higher-order gradient plasticity theory, these variables should contribute to the internal power and free energy.

2.2 Principle of Virtual Power

The principle of virtual power is the assertion that, given any subbody Γ, the virtual power expended on Γ by materials or bodies exterior to Γ (i.e., external power) will be equal to the virtual power expended within Γ (i.e., internal power).

Let $\boldsymbol{n}$ denote the outward unit normal to $\partial\Gamma$. The external expenditure of power is assumed to arise from a macroscopic surface traction t and a macroscopic body force $\boldsymbol{b}$; inertia accompanies the macroscopic motion of the body, which is defined by the virtual velocity vector $\boldsymbol{v}$, and a microtraction $\boldsymbol{m}$ at free surfaces and interfaces (e.g., particle-matrix interface) is a conjugate force for the plastic strain at the interface (physically due to dislocation pileup and transmission). Therefore one can write the external power in the following form:

$$P_{\text{ext}} = \underbrace{\int_{\Gamma} b_i v_i dV + \int_{\partial\Gamma} t_i v_i dA - \int_{\Gamma} \rho \dot{v}_i v_i dV}_{\text{local}} + \underbrace{\int_{\partial\Gamma} m_{ij}\dot{\varepsilon}^p_{ij}\, dA}_{\text{nonlocal}} \tag{15}$$

where ρ is the mass density and $\dot{\boldsymbol{v}}$ is the acceleration vector. The last term in the preceding equation is the new one as compared to the classical (local) form of the external virtual power, which results in a higher-order boundary condition generally consistent with the framework of a gradient-dependent theory. This higher-order boundary condition is imposed on free surfaces and interfaces.

The external power is balanced by an internal expenditure of power (i.e., $P_{\text{ext}} = P_{\text{int}}$), characterized by an elastic stress σ defined over Γ for all time; the back stresses $\boldsymbol{X}$ and $\boldsymbol{S}$ conjugate to $\boldsymbol{\varepsilon}^p$ and $\nabla\boldsymbol{\varepsilon}^p$, respectively, and the drag stresses R, $\boldsymbol{Q}$, and K conjugate to p, ∇p, and e, respectively. Specifically, the internal power is assumed to have the following form:

$$P_{\text{int}} = \underbrace{\int_{\Gamma} \left(\sigma_{ij}\dot{\varepsilon}^e_{ij} + X_{ij}\dot{\varepsilon}^p_{ij} + R\dot{p}\right) dV}_{\text{local}} + \underbrace{\int_{\Gamma} \left(S_{ijk}\dot{\varepsilon}^p_{ij,k} + Q_k\dot{p}_{,k} + K\dot{e}\right) dV}_{\text{nonlocal}} \tag{16}$$

The first integral in Eq. (16) constitutes the definition of the local internal virtual power, whereas the second integral in Eq. (16) is meant to take into

account the large spatial variations in ε^p and p at small length scales. Also, one might argue that the preceding energetic balance might best be characterized through a dependence of P_{int} on p and ∇p and not on ε^p and $\nabla\varepsilon^p$, or vice versa, since all are related through Eqs. (12). But the effects of these variables are different: A dependence of P_{int} on ε^p and $\nabla\varepsilon^p$ gives rise to kinematic hardening, whereas a dependence on p and ∇p gives rise to isotropic hardening. Therefore the stresses $\boldsymbol{X}$ and $\boldsymbol{S}$ introduce kinematic hardening (i.e., the Bauschinger effect), whereas R, $\boldsymbol{Q}$, and K introduce isotropic hardening.

Note that the kinematical fields in Eqs. (15) and (16) are considered to be virtual. Equation (16) is based on the concept that the power expended by each kinematical field is expressible in terms of an associated force system consistent with its own balance [64]. However, these kinematical fields are no longer independent, and therefore special care is taken in the following sections to properly account for their coupling. The nature of this coupling can be determined using the principle of virtual power.

Substituting the relation $\dot{\varepsilon}^e = \dot{\varepsilon} - \dot{\varepsilon}^p$ and the first and second Eqs. (12) and Eq. (13) into Eq. (16) yields

$$P_{\text{int}} = \int_\Gamma \Big[\sigma_{ij}\dot{\varepsilon}_{ij} - (\tau_{ij} - X_{ij} - RN_{ij})\,\dot{\varepsilon}^p_{ij} + (S_{ijk} + (Q_k + K\mathrm{N}_k)\,N_{ij})\,\dot{\varepsilon}^p_{ij,k}\Big]dV \tag{17}$$

where, due to plastic incompressibility, one can easily prove that $\boldsymbol{\sigma} : \dot{\boldsymbol{\varepsilon}}^p = \boldsymbol{\tau} : \dot{\varepsilon}^p$, where $\tau_{ij} = \sigma_{ij} - 1/3\sigma_{kk}\delta_{ij}$ is the deviatoric component of the Cauchy stress tensor, $\boldsymbol{\sigma}$, and δ_{ij} is the Kronecher delta.

Substituting Eq. (2) into Eq. (17) and applying the divergence theorem, one can rewrite Eq. (17) as follows:

$$\begin{aligned} P_{\text{int}} =& -\int_\Gamma \sigma_{ij,j}v_i\,dV - \int_\Gamma \Big[\tau_{ij} - X_{ij} + S_{ijk,k} \\ & -(R - Q_{k,k} - K\mathrm{N}_{k,k} - K_{,k}\mathrm{N}_k)N_{ij}\Big]\dot{\varepsilon}^p_{ij}\,dV \\ & + \int_{\partial\Gamma}\sigma_{ij}n_jv_i dA + \int_{\partial\Gamma}[S_{ijk} + (Q_k + K\mathrm{N}_k)N_{ij}] \\ & \times n_k\dot{\varepsilon}^p_{ij}\,dA \end{aligned} \tag{18}$$

By applying the axiom of equilibrium of the principle of virtual power to the region Γ, $P_{\text{ext}} = P_{\text{int}}$, from Eqs. (15) and (18), one obtains the following equilibrium equation:

$$\begin{aligned} & \int_{\partial\Gamma}(t_i - \sigma_{ij}n_j)\,v_i\,dA + \int_{\partial\Gamma}\Big[m_{ij} - \big(S_{ijk} \\ & + (Q_k + K\mathrm{N}_k)\,N_{ij}\big)n_k\Big]\dot{\varepsilon}^p_{ij}dA \\ & + \int_\Gamma (\sigma_{ij,j} + b_i - \rho\dot{v}_i)\,v_i\,dV \\ & + \int_\Gamma \Big[\tau_{ij} - X_{ij} + S_{ijk,k} - \big(R - Q_{k,k} \\ & - K\mathrm{N}_{k,k} - K_{,k}\mathrm{N}_k\big)N_{ij}\Big]\dot{\varepsilon}^p_{ij}\,dV = 0 \end{aligned} \tag{19}$$

Γ, $\boldsymbol{v}$, and $\dot{\varepsilon}^p$ may be arbitrarily specified if and only if

Macroforce balance

$$\sigma_{ij,j} + b_i = \rho\dot{v}_i \tag{20}$$

Macrotraction condition

$$t_i = \sigma_{ij}n_j \tag{21}$$

Microforce balance

$$\begin{aligned} \tau_{ij} & - X_{ij} + S_{ijk,k} - \big(R - Q_{k,k} - K\mathrm{N}_{k,k} \\ & - K_{,k}\mathrm{N}_k\big)N_{ij} = 0 \end{aligned} \tag{22}$$

Microtraction condition

$$m_{ij} = [S_{ijk} + (Q_k + K\mathrm{N}_k)\,N_{ij}]\,n_k \tag{23}$$

Equation (20) expresses the local static or dynamic equilibrium or the macroforce balance according to [66]. Equation (21) defines the stress vector as the surface density of the forces introduced. It also provides the local macrotraction boundary conditions on forces if the axiom of equilibrium of virtual power is applied to the whole region under consideration, as opposed to arbitrary subregions. One can view the microforce balance, Eq. (22), as the nonlocal plasticity yield condition, as outlined next. Also, one might view the microtraction condition, Eq. (23), as a higher-order condition (or internal boundary condition) augmented by the interaction of dislocations across interfaces, which will be explained subsequently.

2.3 Nonlocal Yield Criterion and Flow Rule

The microforce balance presented in Eq. (22) can be viewed as the nonlocal yield condition, which implies that a yield criterion or a plasticity flow rule

can be directly derived from the principle of virtual power, without making further assumptions. Substituting Eq. (4) into Eq. (22), one can easily write the following expression for the nonlocal plasticity flow rule in Eq. (5):

$$\begin{aligned} N_{ij} &= \frac{\tau_{ij} - X_{ij} + S_{ijk,k}}{R - Q_{k,k} - K\mathrm{N}_{k,k} - K_{,k}\mathrm{N}_k} \\ \Rightarrow \dot{\varepsilon}^p_{ij} &= \dot{p}\frac{\tau_{ij} - X_{ij} + S_{ijk,k}}{R - Q_{k,k} - K\mathrm{N}_{k,k} - K_{,k}\mathrm{N}_k} \end{aligned} \tag{24}$$

Moreover, by taking the Euclidean norm $\| \ \|$ of Eq. (22), one can write

$$\begin{aligned} \big\|\tau_{ij} - X_{ij} + S_{ijk,k}\big\| - \big\|R - Q_{k,k} - K\mathrm{N}_{k,k} \\ - K_{,k}\mathrm{N}_k\big\| \, \|N_{ij}\| = 0 \end{aligned} \tag{25}$$

Since $\|R - Q_{k,k} - K\mathrm{N}_{k,k} - K_{,k}\mathrm{N}_k\| = R - Q_{k,k} - K\mathrm{N}_{k,k} - K_{,k}\mathrm{N}_k$ and $\|N_{ij}\| = 1$, one can then rewrite the preceding expression as the nonlocal yield criterion or the nonlocal plasticity loading surface f:

$$\begin{aligned} f = \|\tau_{ij} - X_{ij} + S_{ijk,k}\| - R + Q_{k,k} \\ + K\mathrm{N}_{k,k} + K_{,k}\mathrm{N}_k = 0 \end{aligned} \tag{26}$$

such that the flow rule in Eq. (24) can also be expressed by

$$\dot{\varepsilon}^p_{ij} = \dot{p}\frac{\tau_{ij} - X_{ij} + S_{ijk,k}}{\|\tau_{mn} - X_{mn} + S_{mnk,k}\|} \tag{27}$$

Comparing Eq. (27) with Eq. (4), one can rewrite the direction of the plastic flow as

$$N_{ij} = \frac{\tau_{ij} - X_{ij} + S_{ijk,k}}{\|\tau_{mn} - X_{mn} + S_{mnk,k}\|} \tag{28}$$

One can notice that the stress $\mathrm{div}\,(\mathbf{S})$ is a back stress quantity giving rise to kinematic hardening, while the forces $\mathrm{div}\,(\mathbf{Q}) = Q_{k,k}$ and $\mathrm{div}\,(K\mathrm{N}_k) = K\mathrm{N}_{k,k} + K_{,k}\mathrm{N}_k$ are giving rise to isotropic hardening. Moreover, if the higher-order gradients are neglected, one can easily retrieve the local plasticity theory.

2.4 Nonlocal Clausius-Duhem Inequality

Utilizing the derived microforce balance, Eq. (22), and the microtraction condition, Eq. (23), in Eq. (18), one can rewrite the expression for the internal power, defined in Eq. (16), as follows:

$$P_{\mathrm{int}} = \int_{\Gamma} \sigma_{ij}\dot{\varepsilon}_{ij}\, dV + \int_{\partial\Gamma} m_{ij}\dot{\varepsilon}^p_{ij}\, dA \tag{29}$$

Comparing the preceding equation with its corresponding local expression (i.e., $P_{\mathrm{int}} = \int_\Gamma \sigma_{ij}\dot{\varepsilon}_{ij} dV$) implies that the long-range (nonlocal) energy interactions can be nonvanishing at particle-matrix interfaces, which is represented by the second term, $\int_{\partial\Gamma} m_{ij}\dot{\varepsilon}^p_{ij} dA$. Hence, according to the notion of Edelen and Laws [105] and Eringen and Edelen [53], the energy term $\int_{\partial\Gamma} m_{ij}\dot{\varepsilon}^p_{ij}\, dA$ is called the *nonlocality energy residual.* Similar arguments have been presented by Polizzotto and Borino [85], who assumed that $\int_{\partial\Gamma} m_{ij}\dot{\varepsilon}^p_{ij}\, dA = 0$ and called it the *insulation condition*, meaning that nonlocal energy is not allowed to flow from any point in Γ to the exterior of the body. This insulation condition yields the following microboundary conditions on plastic interfaces:

$$m_{ij}\dot{\varepsilon}^p_{ij} = 0 \qquad \text{on} \qquad \partial\Gamma^p \tag{30}$$

where $\partial\Gamma^p \subseteq \partial\Gamma$ is the plastic boundary. The preceding equation renders two conditions according to a split of the plastic subdomain boundary into external and internal parts such that $\partial\Gamma^p = \partial\Gamma^p_{\mathrm{int}} \cup \partial\Gamma^p_{\mathrm{ext}}$, as follows [85].

1. One boundary condition is imposed on the external plastic boundary $\partial\Gamma^p_{\mathrm{ext}} \subseteq \partial\Gamma$:

$$m_{ij} = 0 \quad \text{on} \quad \partial\Gamma^p_{\mathrm{ext}} \tag{31}$$

   which gives the so-called Neumann type boundary. This *microtraction-free* (according to the notion of [64]) boundary condition is the simplest form of Eq. (23) and assumes that the moment microtractions m vanish at external surfaces $\partial\Gamma^p_{\mathrm{ext}} = \partial\Gamma^p \cap \partial\Gamma$. Moreover, Eq. (31) places no constraint on the plastic flow and could characterize free dislocation movements across the boundaries. Moreover, in case of external surface tractions, the macrotractions $\boldsymbol{t}$ in Eq. (21) have a value, whereas the microtractions $\boldsymbol{m}$ vanish.

2. The other condition is imposed on the internal plastic boundary $\partial\Gamma^p_{\mathrm{int}}$ such that

$$\dot{\varepsilon}^p_{ij} = 0 \quad \text{on} \quad \partial\Gamma^p_{\text{int}} \tag{32}$$

and gives the so-called continuity boundary condition of Dirichlet type. This condition arises from the consideration that in general, the stress rate $\dot{\sigma}$ is continuous across $\partial\Gamma^p_{\text{int}}$, and thus the related elastic strain rate, $\dot{\boldsymbol{\varepsilon}}^e$, and plastic strain rate, $\dot{\boldsymbol{\varepsilon}}^p$, must be continuous. Moreover, this *microplastic-clamped* (according to the notion of [64]) boundary condition places a constraint on the plastic flow and characterizes the full dislocation blocking and pileup at the interface. Moreover, $\partial\Gamma^p_{\text{int}}$ could characterize a movable elastic-plastic boundary.

However, $\boldsymbol{m}$ is meant to be the driving force at the material internal boundaries (e.g., particle-matrix interface) such that generally, $\boldsymbol{m} \neq 0$. Hence, for an intermediate (i.e., not microtraction-free and not microplastic-clamped) boundary (i.e., $\boldsymbol{m} \neq 0$ on $\partial\Gamma^p_{\text{ext}}$ and $\dot{\varepsilon}^p_{ij} \neq 0$ at $\partial\Gamma^p_{\text{int}}$), one can define the density of the nonlocality energy residual, R, as follows:

$$\int_\Gamma \mathrm{R}\, dV = \int_{\partial\Gamma} m_{ij}\dot{\varepsilon}^p_{ij} dA \tag{33}$$

Therefore, if one neglects the interior surface energy that results from dislocation interactions at the internal boundaries (e.g., internal boundaries at inclusions), the insulation condition of Polizzotto (e.g., [85, 86]) can be expressed as

$$\int_\Gamma \mathrm{R}\, dV = 0 \tag{34}$$

By substituting the expression for $\boldsymbol{m}$ from Eq. (23) into Eq. (33) and applying the divergence theorem, one obtains

$$\int_\Gamma \mathrm{R}\, dV = \int_\Gamma \left([S_{ijk} + (Q_k + K\mathrm{N}_k)\, N_{ij}]\, \dot{\varepsilon}^p_{ij} \right)_{,k} dV \tag{35}$$

from which R is given by

$$\begin{aligned} \mathrm{R} &= \left([S_{ijk} + (Q_k + K\mathrm{N}_k)\, N_{ij}]\, \dot{\varepsilon}^p_{ij} \right)_{,k} \\ &= [S_{ijk,k} + (Q_{k,k} + K\mathrm{N}_{k,k} + K_{,k}\mathrm{N}_k) N_{ij}] \dot{\varepsilon}^p_{ij} \\ &\quad + [S_{ijk} + (Q_k + K\mathrm{N}_k)\, N_{ij}]\, \dot{\varepsilon}^p_{ij,k} \end{aligned} \tag{36}$$

One considers here a purely mechanical theory (isothermal conditions are assumed) based on the requirement that the rate of change in the total free energy should be less than or equal to the power done by external forces [65]. If one denotes $\rho\Psi$ as the specific free energy, this requirement takes the form of a free energy inequality:

$$\int_\Gamma \dot{\Psi} dV \leq P_{\text{ext}} \tag{37}$$

Substituting the virtual work balance equation, $P_{\text{ext}} = P_{\text{int}}$, into Eq. (37) along with the new form of the internal power presented in Eq. (29), one can write the following thermodynamic restriction in a point-wise form:

$$\sigma_{ij}\dot{\varepsilon}_{ij} - \dot{\Psi} + \mathrm{R} \geq 0 \tag{38}$$

The inequality in Eq. (38) is termed here the *nonlocal Clausius-Duhem inequality*, differing from its classical counterpart only in the presence of the nonlocality residual R. This inequality holds everywhere in Γ, but $\mathrm{R} = 0$ at material points in the elastic zone. Moreover, for a homogeneous strain distribution $\mathrm{R} = 0$, one retains the classical (local) Clausius-Duhem inequality.

Next, the nonlocal Clausius-Duhem inequality in Eq. (38) will be employed for deriving the thermodynamic restrictions and constitutive equations.

2.5 Helmholtz Free Energy and Interfacial Effects

The hardening in plasticity is introduced as hidden independent internal state variables in the thermodynamic state potential. The Helmholtz free specific energy function Ψ is considered as the thermodynamic state potential, depending on both *observable* and *internal* state variables. However, before giving its definition, a choice must be made with respect to the nature of the state variables. Here one chooses the same state variables that contribute to the internal power; namely, $\boldsymbol{\varepsilon}^e$, $\boldsymbol{\varepsilon}^p$, p, $\nabla\boldsymbol{\varepsilon}^p$, ∇p, and e. Therefore it is argued here that these variables must appear in the definition of Ψ if they do contribute to the internal power expression. Moreover, plastic deformation is mainly carried by dislocations within the bulk (e.g., individual grains). Dislocations can move through the crystal grains and can interact with each other. Interfaces (particle-matrix interfaces and grain boundaries) often hinder their

transmission, creating a dislocation pileup at the interface and thereby making the material harder to deform. Therefore, additionally to the bulk free energy, an interfacial energy ϕ (free energy per unit area) exists in the plastic boundary layer surrounding the inclusion (see Fig. 2). This interfacial energy introduces an interfacial resistance against dislocation motion, emission, and transmission. Therefore one can define the total free energy to have the following additive form:

$$\begin{aligned}\Psi = \Psi^e\left(\varepsilon^e_{ij}\right) + \Psi^p\left(\varepsilon^p_{ij}, p, \varepsilon^p_{ij,k}, p_{,k}, e\right) \\ +\frac{1}{\ell_I}\phi\left(\varepsilon^p_{ij}\right)\end{aligned} \tag{39}$$

where Ψ^e is the elastic free energy, Ψ^p is the plastic free energy, and ℓ_I is another microstructural length-scale parameter (besides the bulk length-scale parameter ℓ in Eq. (14)), which represents the boundary layer thickness. The reader is referred to [102] for more detail on the physical nature of ℓ_I and to [80, 96, 97] for the physical nature of ℓ. Therefore both Ψ^e and Ψ^p are free energies within the bulk of the material, and ϕ is an interfacial energy within the boundary layer. The latter is dependent on $\boldsymbol{\varepsilon}^p$ at the interface ($\boldsymbol{\varepsilon}^p|_{\partial\Gamma^p} = \boldsymbol{\varepsilon}^{p(I)}$). Therefore continuity of the strain field requires that both the interfacial plastic strain $\boldsymbol{\varepsilon}^{p(I)}$ and the bulk plastic strain $\boldsymbol{\varepsilon}^p$ be identical at the interface such that the boundary layer deforms plastically as the adjacent bulk material. The dependence of ϕ on $\nabla\boldsymbol{\varepsilon}^p$ will be investigated in a future work.

It is noteworthy that the inclusion of the interfacial free energy function ϕ directly into the definition of the Helmholtz free energy in Eq. (39) allows the interfacial layer or boundary surface to dissipate energy during interfacial plasticity similarly to the bulk of the material. The works of Gudmundson [69], Aifantis and Willis [24, 100], Fredricksson and Gudmundson [101], Abu Al-Rub et al. [70], and Abu Al-Rub [102] assume nondissipative interfaces.

It will be shown next that the microtraction stress m in the microscopic boundary condition in Eq. (23) is related to the interfacial energy ϕ. Taking the time derivative of Eq. (39) with respect to its internal state variables yields

$$\begin{aligned}\dot{\Psi} = \frac{\partial\Psi^e}{\partial\varepsilon^e_{ij}}\dot{\varepsilon}^e_{ij} + \frac{\partial\Psi^p}{\partial\varepsilon^p_{ij}}\dot{\varepsilon}^p_{ij} + \frac{\partial\Psi^p}{\partial p}\dot{p} + \frac{\partial\Psi^p}{\partial\varepsilon^p_{ij,k}}\dot{\varepsilon}^p_{ij,k} \\ +\frac{\partial\Psi^p}{\partial p_{,k}}\dot{p}_{,k} + \frac{\partial\Psi^p}{\partial e}\dot{e} + \frac{1}{\ell_I}\frac{\partial\phi\left(\varepsilon^p\right)}{\partial\varepsilon^{p(I)}_{ij}}\dot{\varepsilon}^{p(I)}_{ij}\end{aligned} \tag{40}$$

Making use of Eqs. (12), (13), and (23) in Eq. (40), and applying the nonlocal Clausius-Duhem inequality from Eq. (38), along with Eq. (36), one obtains the following thermodynamic laws:

$$\sigma_{ij} = \rho\frac{\partial\Psi^e}{\partial\varepsilon^e_{ij}}, \quad X_{ij} = \rho\frac{\partial\Psi^p}{\partial\varepsilon^p_{ij}}, \quad R = \sigma_y + \rho\frac{\partial\Psi^p}{\partial p} \tag{41}$$

$$S_{ijk} = \rho\frac{\partial\Psi}{\partial\varepsilon^p_{ij,k}}, \quad Q_k = \rho\frac{\partial\Psi}{\partial p_{,k}}, \quad K = \rho\frac{\partial\Psi}{\partial e} \tag{42}$$

$$m_{ij} = \frac{\partial\phi\left(\varepsilon^p\right)}{\partial\varepsilon^{p(I)}_{ij}} \tag{43}$$

where σ_y is the scale-independent yield strength. Note that in obtaining Eqs. (41), it is assumed that $X = \rho\Psi^p/\boldsymbol{\varepsilon}^p$ and $R - \sigma_y = \rho\partial\Psi^p/\partial p$ such that $\boldsymbol{X} = 0$ and $R = \sigma_y$ at initial yielding. For more detail, the reader is referred to [70]. Moreover, according to Eq. (43), $\phi = 0$ designates a free surface where dislocations are allowed to escape (i.e., Eq. (31)), whereas $\phi \to \infty$ designates a microclamped interface (i.e., Eq. (32)) where dislocations are not allowed to penetrate. Hence, for intermediate interfaces where some dislocations are blocked and some can escape, finite values for ϕ are obtained.

To develop equations amenable to the analysis and computation, we will now consider an example for the definition of the Helmholtz free energy function Ψ and the interfacial energy function ϕ. One can assume decoupling between the elastic behavior and plasticity hardening (i.e., separable material) such that both Ψ^e and Ψ^p, which appear in Eq. (39) can be assumed to have the following quadratic analytical form:

$$\rho\Psi^e = \frac{1}{2}\varepsilon^e_{ij}E_{ijkl}\varepsilon^e_{kl} \tag{44}$$

$$\begin{aligned}\rho\Psi^p = \frac{1}{2}a_1\varepsilon^p_{ij}\varepsilon^p_{ij} + \frac{1}{2}a_2p^2 + \frac{1}{2}a_3\varepsilon^p_{ij,k}\varepsilon^p_{ij,k} \\ +\frac{1}{2}a_4p_{,k}p_{,k} + \frac{1}{2}a_5e^2\end{aligned} \tag{45}$$

where E is the symmetric fourth-order elastic stiffness tensor and a_i ($i = 1 - 5$) are material constants. However, utilizing the relations

$$p^2 = \varepsilon^p_{ij}\varepsilon^p_{ij}, \quad e^2 = \varepsilon^p_{ij,k}\varepsilon^p_{ij,k} = p_{,k}p_{,k} \tag{46}$$

respectively, from Eqs. (3) and (9) for proportional loading, one can equivalently write Eq. (45) as

$$\rho\Psi^p = \frac{1}{2}\left(a_1 + a_2\right)p^2 + \frac{1}{2}\left(a_3 + a_4 + a_5\right)e^2 \tag{47}$$

Moreover, by assuming that the hardening moduli $h = a_1 + a_2$ and $h\ell^2 = a_3 + a_4 + a_5$, one can rewrite Eq. (47) as

$$\rho\Psi^p = \frac{1}{2}h\left(p^2 + \ell^2 e^2\right) = \frac{1}{2}hE^2 \tag{48}$$

where the generalized effective plastic strain E is given by Eq. (14) for proportional loading.

Now, one can obtain the Cauchy stress from Eqs. (41) and (44) such that

$$\sigma_{ij} = E_{ijkl}\varepsilon^e_{kl} = E_{ijkl}\left(\varepsilon_{kl} - \varepsilon^p_{kl}\right) \tag{49}$$

and the local and nonlocal conjugate forces, by making use of Eqs. (41) and (42)(, respectively, as follows:

$$X_{ij} = h\varepsilon^p_{ij} \tag{50}$$

$$R = \sigma_y + hp \tag{51}$$

$$S_{ijk} = h\ell^2\varepsilon^p_{ij,k} \tag{52}$$

$$Q_k = h\ell^2 p_{,k} \tag{53}$$

$$K = h\ell^2 e \tag{54}$$

Moreover, substituting Eqs. (52)–(54) into the yield function f, Eq. (26), one can then write

$$\begin{aligned} f = {} & \|\tau_{ij} - X_{ij} + S_{ijk,k}\| - \gamma - h \\ & \times \left[p - \ell^2\left(\nabla^2 p + \|\nabla_i p\|\,\mathrm{N}_{k,k} + e_{,k}\mathrm{N}_k\right)\right] = 0 \end{aligned} \tag{55}$$

with

$$S_{ijk,k} = h\ell^2\nabla^2\varepsilon^p_{ij} \tag{56}$$

where ∇^2 designates the Laplacian operator and ∇_k designates the first gradient vector.

For monotonic and proportional loading (in the case of isotropic hardening), one can easily show, by using Eqs. (9) and (10), that the last two terms on the left-hand side of Eq. (55) can be reduced to

$$\|\nabla_i p\|\,\mathrm{N}_{k,k} + e_{,k}\mathrm{N}_k = \nabla^2 p \tag{57}$$

such that f can be given by

$$\begin{aligned} f = {} & \underbrace{\left\|\tau_{ij} - h\varepsilon^p_{ij} + h\ell^2\nabla^2\varepsilon^p_{ij}\right\|}_{\text{effective von Mises stress}} \\ & - \underbrace{\gamma - hp + 2h\ell^2\nabla^2 p}_{\text{isotropic hardening function}} = 0 \end{aligned} \tag{58}$$

Thus this theory shows that the Laplacian of the effective plastic strain contributes to the size of the yield surface (isotropic hardening) and the Laplacian of the plastic strain contributes to the movement of the center of the yield surface (kinematic hardening). It is also noteworthy that the present formulation links hardening to the gradients of plastic strain $\nabla\boldsymbol{\varepsilon}^p$ and the effective plastic strain ∇p and, respectively, not to $\nabla^2\boldsymbol{\varepsilon}^p$ and $\nabla^2 p$, consistent with basic notions of the role of the net Burgers vector and the geometrically necessary dislocations. Instead, $\nabla^2\boldsymbol{\varepsilon}^p$ and $\nabla^2 p$ emerge in the resulting field equations as by-products of the more fundamental role of the plastic strain gradients.

The nonlocal yield function in Eq. (58) should be supplemented by the microscopic boundary conditions derived in Eqs. (23) and (43). Abu Al-Rub [102] showed, after examining several mathematical forms of the interfacial energy, that the following expression for ϕ gives qualitatively good predictions of yield strength and the strain hardening increase with decreasing size for micro/nanostructured metallic systems, such that

$$\phi = \ell_I\left[\sigma_y\left\|\varepsilon^{p(I)}_{ij}\right\| + \frac{1}{2}h\left\|\varepsilon^{p(I)}_{ij}\right\|^2\right] \quad \text{on} \quad \partial\Gamma^p \tag{59}$$

where $\|\varepsilon^{p(I)}_{ij}\| = \sqrt{\varepsilon^{p(I)}_{ij}\varepsilon^{p(I)}_{ij}}$ is a measure of the plastic strain accumulation at the interface; $\gamma = \ell_I\sigma_y$ is the interfacial yield strength, analogous to the bulk yield strength σ_y, which characterizes the yield strength of the boundary layer at the particle-matrix interface; and $\beta = \ell_I h$ is the interfacial hardening, analogous to the bulk hardening modulus h, which characterizes the hardening during the transmission of dislocations across the interface. Therefore, if $\gamma = 0$, the interface would yield at the same time as the bulk yields, and consequently, the interfacial effect is controlled by the interfacial hardening parameter β, whereas, if $\beta = 0$, the interface would yield at a different time as the bulk yields, but the interface would not harden. Note that both the stiffness and hardening of the interface are altered simultaneously by the length scale ℓ_I. Therefore Eq. (59) ensures that if $\ell_I = 0$, the interface will behave like a free surface, and one would obtain a micro-free boundary condition (i.e., $\boldsymbol{m} = 0$). On the other hand, if $\ell_I \to \infty$, then it would represent a condition for fully constrained dislocation movement at the interface, and one would obtain a microclamped boundary condition (i.e., $\boldsymbol{\varepsilon}^{p(I)} = 0$).

This is consistent with the requirement that when $\varphi \to \infty$, $\boldsymbol{\varepsilon}^{p(I)} = 0$, and when $\varphi \to 0$, $\boldsymbol{m} = 0$.

The microtraction stress at the interface, $\boldsymbol{m}$, can then be obtained from Eqs. (43) and (59) as

$$m_{ij} = \ell_I \left[\sigma_y \frac{\varepsilon_{ij}^{p(I)}}{\left\| \varepsilon_{mn}^{p(I)} \right\|} + h \varepsilon_{ij}^{p(I)} \right] \quad \text{on} \quad \partial\Gamma^p \tag{60}$$

such that for $\boldsymbol{\varepsilon}^{p(I)} = 0$, $m_{ij} = \pm \ell_I \sigma_y \delta_{ij}$. The microtraction stress is thus collinear with the plastic strain at the interface.

By taking the Euclidean norm of Eq. (60), one can write an interfacial yield condition, $f^{(I)}$, similar to the yield condition for the bulk, f, such that

$$f_I = \|m_{ij}\| - \ell_I \left(\sigma_y + h \left\| \varepsilon_{ij}^{p(I)} \right\| \right) = 0 \quad \text{on} \quad \partial\Gamma^p \tag{61}$$

where the microtraction stress $\boldsymbol{m}$ at the interface is given by Eq. (23) such that after substituting Eqs. (52)–(54), and Eqs. (10), (12), and (13) for proportional loading, one can express $\boldsymbol{m}$ as follows:

$$m_{ij} = 3h\ell^2 \varepsilon^p_{ij,k} n_k \quad \text{on} \quad \partial\Gamma^p \tag{62}$$

The interfacial yield condition, Eq. (61), needs to be satisfied at the interface and can be used to determine the stress at which the interface begins to deform plastically and harden. This means that if $||m_{ij}|| < \ell_I \sigma_y$, then the interface is impenetrable to dislocations, and no plastic deformation is developed at the interface. Once $||m_{ij}|| = \ell_I \sigma_y$, the interface yields plastically such that the plastic strain there is not zero, which implies that interfacial hardening is activated. Then the interface continues to deform, as long as $||m_{ij}|| \geq \ell_I \sigma_y$, in a linear hardening mode characterized by $\ell_I h$ such that plastic strain accumulates in both the interface and the bulk interior through dislocation motion and multiplication.

3. PHYSICAL INTERPRETATION OF THE MATERIAL LENGTH SCALES

In spite of the crucial importance of the bulk (or matrix) material length scale ℓ in the gradient theory (see Eq. (58)), very few studies have focused on the physical origin of this length-scale parameter. In the literature, the microstructural origin of ℓ is rarely clear, and its value is usually a free parameter. In fact, the full utility of the gradient-dependent theory hinges on one's ability to identify accurate values for ℓ. More important is the difficulty of carrying out truly definitive experiments on critical aspects of the evolution of the dislocation, crack, and void structures that reveal the physical nature of ℓ. Abu Al-Rub and Voyiadjis [96] have concluded that the determination of ℓ should be based on information from micromechanical, gradient-dominant tests such as micro- and nanoindentation tests. Initial attempts have been made by Abu Al-Rub and Voyiadjis [96, 97] and Abu Al-Rub [98] to relate ℓ to the microstructure of metallic matrices and present a dislocation-based approach for the analytical identification of ℓ and show that ℓ is proportional to the *mean free-path for dislocation motion*, and is not constant (or fixed), but varies with the material microstructural features (e.g., the mean grain size in polycrystals or the mean particle size in particle-reinforced composites) and the course of plastic deformation. Moreover, Abu Al-Rub and Voyiadjis [97] have shown for dynamic problems that ℓ decreases with increasing plastic strain, increasing strain hardening rates, increasing strain rate, and decreasing temperature, and its value is on the order of micrometers. Based on dislocation mechanics and comparisons with size-effect data from many microdeformation experiments on small-scale metallic specimens, Voyiadjis and Abu Al-Rub [99] have proposed the following expression for ℓ:

$$\ell = \frac{d\,D}{D + d\,p^{1/m}} \tag{63}$$

where d is the mean grain size or mean particle (inclusion) size, D is the mean interparticle spacing in particle-reinforced composites or other characteristic sizes, p is the effective plastic strain, and m is the strain-hardening exponent in power-law hardening plasticity. This equation shows that ℓ decreases with the effective plastic strain, increases with the grain size or inclusion size, decreases with the ratio of D/d, and decreases with the strain-hardening rate. It also shows that ℓ decreases from an initial value $\ell = d$ at yielding to a final value $\ell \to 0$, which corresponds to the classical local plasticity at very large values of D, d, or p.

On the other hand, based on Taylor's hardening law, Nix and Gao [60] have expressed ℓ in terms of macroscopic and microscopic quantities such that

$$\ell = 18\alpha^2 \left(\frac{G}{\sigma_y}\right)^2 b \tag{64}$$

where α is an empirical parameter (ranging from 0.1 to 0.5), G is the shear modulus, σ_y is the yield strength, and b is the magnitude of Burgers vector. However, this expression gives constant values for ℓ, which is different than the expression in Eq. (63).

In this article, an additional material length scale is introduced, which is the interfacial material length scale ℓ_I (see Eq. (61)). Recently, Abu Al-Rub [102] studied the physical origin of ℓ_I and derived an expression for it based on the misorientation or misfit dislocation density at grain/particle/phase boundaries such that

$$\ell_I = \frac{\sqrt{2}}{4\pi\,(1-\nu)} b \left(\frac{G}{\sigma_y}\right) \log\left(\frac{eb}{2\pi r_0}\right) \tag{65}$$

where ν is the Poisson's ratio, e is the base of the natural logarithm, and r_0 is the radius of the dislocation core. This expression gives values on the range of interface thicknesses (i.e., a few nanometers) [102].

Obviously, critical microdeformation experiments, microstructural characterization techniques, and atomistic and discrete dislocation simulations on the dislocation activity within the bulk and at interfaces are highly needed to check the validity of the preceding expressions for the material length scales.

4. APPLICATION TO METALLIC MATRICES WITH DISPERSED HARD/SOFT PARTICLES

The proposed higher-order gradient plasticity has been implemented in the finite element code Abaqus via the user material subroutine UMAT. The direct and simple numerical implementation method for gradient-dependent theories, as presented by Abu Al-Rub and Voyaidjis [52], has been utilized for calculating the plastic strain gradients. Therefore the reader is referred to [52] for more detail about the finite element implementation of the gradient plasticity theories.

The implemented higher-order gradient plasticity is employed to handle size effects in advanced metal matrix composites with dispersed hard (e.g., ceramic), soft (e.g., metallic), or intermediate compliant inclusions (particles) under macroscopically uniform uniaxial stress σ_0, where d is the particle size (see Fig. 2). For simplicity, the particles are assumed to be uniformly distributed and the matrix material is taken to be linearly hardening elastoplastic.

The ratio ℓ_I/ℓ characterizes the nondimensional particle-matrix interfacial strength and hardening. Therefore different particle-matrix interfaces are characterized by different ℓ_I/ℓ values. Moreover, different particle sizes are characterized by different ratios of ℓ/d. Therefore, depending on the value of the bulk length-scale parameter ℓ and the particle size d (in other words, depending on the ratio of ℓ/d), one can describe the effect of macro-, meso-, micro-, and nanoscales within the current framework. For example, if ℓ is set constant and equal to $1\mu\text{m}$, then a ratio of $\ell/d < 1$ describes particles of greater than a micron in size, whereas if $\ell/d > 1$, the submicron size of particles is described. Results in Figs. 3 and 4 are presented for $h/E = 0.2$, where E is the Young's modulus. Different particle sizes are represented by ℓ/d = 0.1, 0.5, and 1 (for micron and greater particles), and 1.5 and 2 (for submicron particles). The particle volume fraction is taken to be constant at 12.5%. Therefore the focus is on the particle size effect.

In Figs. 3(a) and 3(b), the applied stress σ_0 (normalized with respect to the matrix yield strength σ_y) versus the calculated average strain (normalized with respect to the yield strain $\varepsilon_y = \sigma_y/E$) is shown for two particle-matrix interface conditions (i.e., depending on the value of the interfacial length scale ℓ_I): an intermediate interface with $\ell_I/\ell = 0.5$ (Fig. 3(a)) and a stiff interface with $\ell_I/\ell = 1$ (Fig. 3(b)). It can be seen from Fig. 3(a) or Fig. 3(b) that both the initial macroscopic yield strength (σ_Y in Fig. 4(a)) and the tangent hardening modulus ($E^T = d\sigma/d\varepsilon$ in Fig. 4(b)) increase as the particle size d decreases. However, a higher increase in both σ_Y and E^T is seen for a stiffer particle-matrix interface (Fig. 3(b)) as compared to a compliant interface (Fig. 2).

Since the ability of the particle-matrix interface in resisting dislocation emission at the interface and transmission through the interface is characterized by the level of interfacial energy (or equivalently, ℓ_I), the variations of the macroscopic yield strength of the composite $\sigma_Y\,\sigma_Y$ and the strain hardening rate E^T with the particle size d are shown in Figs. 4(a) and 4(b) for different values of the interfacial length scale ℓ_I. Note that $\ell_I/\ell \to \infty$ corresponds to

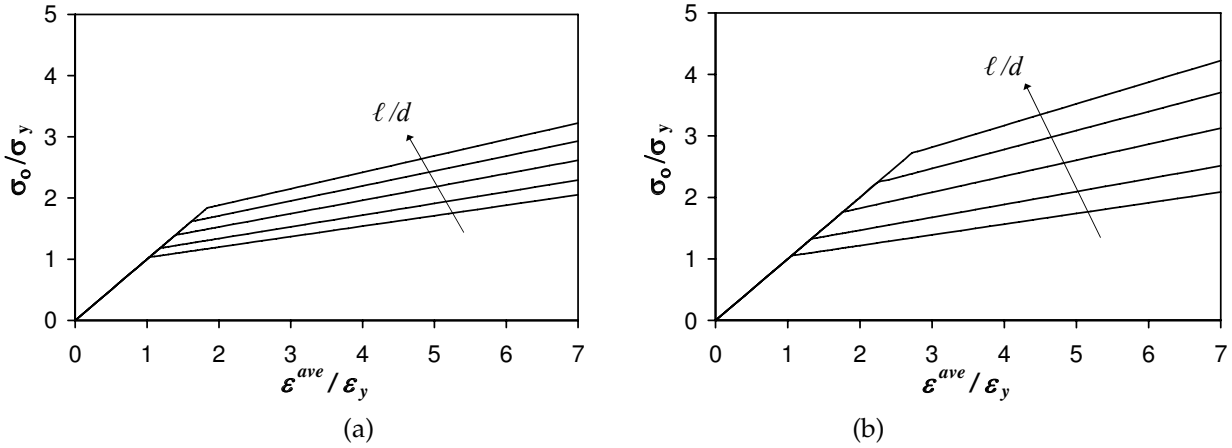

FIGURE 3. Normalized stress-strain relations for **(a)** compliant inclusions ($\ell_I/\ell = 0.5$) and **(b)** hard inclusions ($\ell_I/\ell = 1$). Different particle sizes d are represented by $\ell/d = 0.1$, 0.5, 1, 1.5, 2, where ℓ is the bulk (or matrix) length scale and ℓ_I is the interfacial length scale

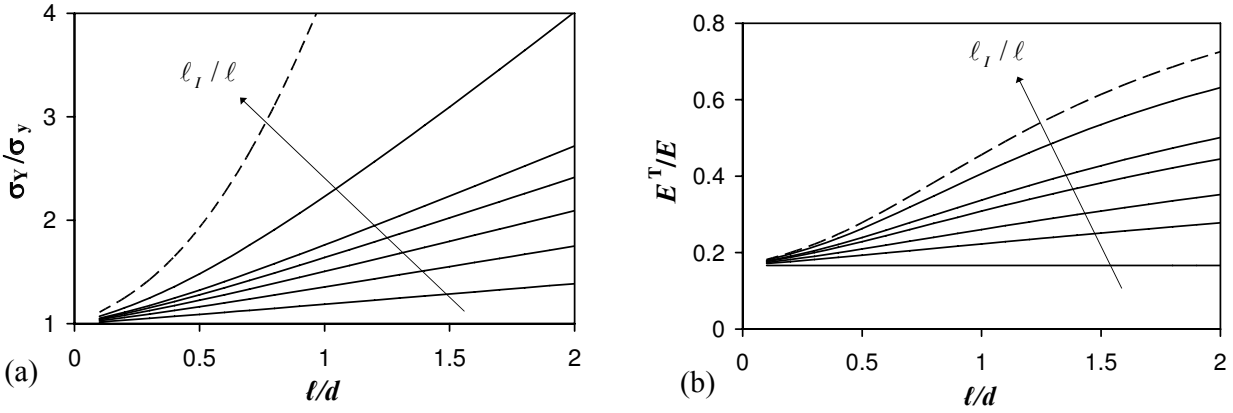

FIGURE 4. (a) Normalized macroscopic yield strength of the composite σ_Y and **(b)** tangent hardening modulus E^T versus particle size d for different particle-matrix interfacial energy characterized by $\ell_I/\ell = 0.2$, 0.4, 0.6, 0.8, 1, 2, and ∞. The dashed line is for a rigid particle (i.e., $\ell_I/\ell \to \infty$), where ℓ is the bulk (or matrix) length scale and ℓ_I is the interfacial length scale

a rigid particle for which dislocations are not allowed to cross over the interface. In this case, d alone (represented by the ratio ℓ/d) controls both the overall yield strength and the strain hardening rate, whereas for compliant or intermediate interfaces, both d and ℓ_I control the overall yield strength and the strain hardening rate. Furthermore, it can be seen from Fig. 4(b) that for very small d (i.e., $\ell/d \to \infty$), the magnitude of the tangent modulus E^T gets closer to the magnitude of the elastic modulus E.

More detailed parametric studies on the effectiveness of the different parameters in the proposed gradient theory and comparisons with available experimental data in the literature of size effects in advanced metal matrix composites will be presented in a future work. The focus will also be on combining interfacial hardening (as presented in this ar-

ticle) and interfacial softening (e.g., using cohesive zone models) to study the impact of particle size and interfacial properties on the ultimate strength, failure, and ductility of metal matrix composites reinforced with dispersed particles at decreasing microstructural length scales.

5. CONCLUSIONS

A thermodynamic-based theory for small strain gradient plasticity is developed by introducing gradients for variables associated with kinematic and isotropic hardening. This theory is a three nonlocal parameter theory that takes into consideration large variations in the plastic strain, large variations in the accumulated plastic strain, and accumulation of plastic strain gradients. Thermodynamically consistent equations for the nonlocal plasticity yield a criterion, and interfacial yieldlike condition are derived based on the principle of virtual power and the laws of thermodynamics. It is shown that the presence of higher-order gradients in the plastic strain enforces the presence of a corresponding history variable brought by the accumulation of the plastic strain gradients. The latter is similar to the history variable in the classical plasticity theory such that none of the plastic strain or the effective plastic strain can exist without the other. Gradients in the plastic strain introduce anisotropy in the form of kinematic hardening and are attributed to the net Burgers vector, whereas gradients in the accumulation of the plastic strain introduce isotropic hardening, attributed to the additional storage of GNDs.

It is shown that the higher-order microscopic boundary conditions that result from the higher-order gradient-dependent framework can be related to the surface/interfacial energy at free surfaces and interfaces. This main contribution of the article can be used in explaining the particle size effect and the effect of particle-matrix interfacial strength and hardening properties on the overall yield strength and strain hardening rates in metal matrix composites. The interfacial yield strength explains the increase in onset of plasticity (i.e., the yield strength) of the composite as the particle size decreases, whereas the interfacial hardening (i.e., the ability of the interface to resist dislocation transmission across the interface) explains the further increase in strain hardening rate, and ultimately, the ultimate strength of the composite, as the particle size decreases. Both interfacial yield strength and interfacial hardening properties are scaled by an interfacial length scale, which is related to the boundary layer thickness at the interface.

Also, it is concluded that for rigid particles, the bulk (i.e., the metal matrix) length scale controls the particle size effect, whereas for soft and intermediate particles, the interfacial length scale controls the particle size effect.

Another future development is greatly needed that will combine interfacial/bulk hardening and softening to explain the particle size effect on the ultimate strength, ductility, and failure of advanced particle reinforced metal matrix composites.

ACKNOWLEDGMENTS

The work reported in this article is supported by a joint grant from the U.S. National Science Foundation and the U.S. Department of Energy (NSF#0728032). Also, this research is supported by a grant from the U.S. Army Research Office. These sources of support are gratefully acknowledged.

REFERENCES

1. Argon, A. S., Im, J., and Safoglu, R., Cavity formation from inclusions in ductile fracture. *Metall. Trans. A.* **6**:825–837, 1975.
2. Llorca, J., Needleman, A., and Suresh, S., An analysis of the effects of matrix void growth on deformation and ductility in metal-ceramic composites. *Acta Metall. Mater.* **39**:2317–2335, 1991.
3. Zhao, D., Tuler, F. R., and Lloyd, D. J., Fracture at elevated temperatures in a particle reinforced composite. *Acta Metall. Mater.* **42**:2525–2533, 1994.
4. Dierickx, P., Verdu, C., Reynaud, A., and Fougeres, R., A study of physico-chemical mechanisms responsible for damage of heat treated and as-cast ferritic spheroidal graphite cast irons. *Script. Metall.* **34**:261–268, 1996.
5. Xue, Z., Huang, Y., and Li, M., Particle size effect in metallic materials: A study by the theory of mechanism-based strain gradient plasticity. *Acta Mater.* **50**:149–160, 2002.
6. Gall, K., Yang, N., Horstemeyer, M. F., McDowell, D. L., and Fan, J., Debonding and fracture of

Si particles during the fatigue of a cast Al-Si alloy. *Metall. Mater. Trans. A.* **30**:3079–3088, 1999.

7. Horstemeyer, M. F., Ramaswamy, S., and Negrete, M., Using a micromechanical finite element parametric study to motivate a phenomenological macroscale model for void/crack nucleation in aluminum with a hard second phase. *Mech. Mater.* **35**:675–687, 2003.
8. Hao, S., Liu, W. K., Moran, B., Vernerey, F., and Olson, G. B., Multi-scale constitutive model and computational framework for the design of ultra-high strength, high toughness steels. *Comput. Methods Appl. Mech. Eng.* **193**:1865–1908, 2004.
9. Bandstra, J. P., Koss, D. A., Geltmacher, A., Matic, P., and Everett, R. K., Modeling void coalescence during ductile fracture of a steel. *Mater. Sci. Eng. A.* **366**:269–281, 2004.
10. Babout, L., Maire, E., and Fougeres, R., Damage initiation in model metallic materials: X-ray tomography and modeling. *Acta Mater.* **52**:2475–2487, 2004.
11. Lee, J. H., Shishidou, T., Zhao, Y. J., Freeman, A. J., and Olson, G. B., Strong interface adhesion in Fe/TiC. *Philos. Mag.* **85**:3683–3697, 2005.
12. Tan, H., Huang, Y., Liu, C., and Geubelle, P. H., The effect of nonlinear interface debonding on the constitutive model of composite materials. *Int. J. Multiscale Comput. Eng.* **4**:147–167, 2006.
13. McVeigha, C., Vernereya, F., Liu, W. K., and Brinson, L. C., Multiresolution analysis for material design. *Comput. Methods Appl. Mech. Eng.* **195**:5053–5076, 2006.
14. McVeigha, C., Vernereya, F., Liu, W. K., Morana, B., and Olson, G. B., An interactive micro-void shear localization mechanism in high strength steels. *J. Mech. Phys. Solids.* **55**:225–244, 2007.
15. Lloyd, D. J., Particle reinforced aluminum and magnesium matrix composites. *Int. Mater. Rev.* **39**:1–23, 1994.
16. Rhee, M., Hirth, J. P., and Zbib, H. M., A superdislocation model for the strengthening of metal matrix composites and the initiation and propagation of shear bands. *Acta Metall. Mater.* **42**:2645–2655, 1994.
17. Zhu, H. T., and Zbib, H. M., Flow strength and size effect of an Al-Si-Mg composite model system under multiaxial loading. *Script. Metall. Mater.* **32**:1895–1902, 1995.
18. Nan, C.-W., and Clarke, D. R., The influence of particle size and particle fracture on the elastic/plastic deformation of metal matrix composites. *Acta Mater.* **44**:3801–3811, 1996.
19. Kiser, M. T., Zok, F. W., and Wilkinson, D. S., Plastic flow and fracture of a particulate metal matrix composite. *Acta Mater.* **44**:3465–3476, 1996.
20. Kouzeli, M., and Mortensen, A., Size dependent strengthening in particle reinforced aluminium. *Acta Mater.* **50**:39–51, 2002.
21. Ashby, M. F., The deformation of plastically non-homogenous alloys. *Philos. Mag.* **21**:399–424, 1970.
22. Chen, S., and Wang, T. C., Size effects in the particle-reinforced metal-matrix composites. *Acta Mech.* **157**:113–127, 2002.
23. Fleck, N. A., and Willis, J. R., Bounds and estimates for the effect of strain gradients upon the effective plastic properties of an isotropic two phase composite. *J. Mech. Phys. Solids.* **52**:1855–1888, 2004.
24. Aifantis, K. E., and Willis, J. R., The role of interfaces in enhancing the yield strength of composites and polycrystals. *J. Mech. Phys. Solids.* **53**:1047–1070, 2005.
25. Stolken, J. S., and Evans, A. G., A microbend test method for measuring the plasticity length-scale. *Acta Mater.* **46**:5109–5115, 1998.
26. Huang, H., and Spaepen, F., Tensile testing of free-standing Cu, Ag and Al thin films and Ag/Cu multilayers. *Acta Mater.* **48**:3261–3269, 2000.
27. Shrotriya, P., Allameh, S. M., Lou, J., Buchheit, T., and Soboyejo, W. O., On the measurement of the plasticity length scale parameter in LIGA nickel foils. *Mech. Mater.* **35**:233–243, 2003.
28. Haque, M. A., and Saif, M. T. A., Strain gradient effect in nanoscale thin films. *Acta Mater.* **51**:3053–3061, 2003.

29. Espinosa, H. D., Prorok, B. C., and Peng, B., Plasticity size effects in free-standing submicron polycrystalline FCC films subjected to pure tension. *J. Mech. Phys. Solids.* **52**:667–689, 2004.

30. Simons, G., Weippert, C., Dual, J., and Villain, J., Size effects in tensile testing of thin cold rolled and annealed Cu foils. *Mater. Sci. Eng. A.* **416**:290–299, 2006.

31. Stelmashenko, N. A., Walls, M. G., Brown, L. M., and Milman, Y. V., Microindentation on W and Mo oriented single crystals: An STM study. *Acta Metall. Mater.* **41**:2855–2865, 1993.

32. DeGuzman, M. S., Neubauer, G., Flinn, P., and Nix, W. D., The role of indentation depth on the measured hardness of materials. *Mater. Res. Symp. Proc.* **308**:613–618, 1993.

33. Ma, Q., and Clarke, D. R., Size dependent hardness in silver single crystals. *J. Mater. Res.* **10**:853–863, 1995.

34. Poole, W. J., Ashby, M. F., and Fleck, N. A., Micro-hardness of annealed and work-hardened copper polycrystals. *Script. Mater.* **34**:559–564, 1996.

35. McElhaney, K. W., Valssak, J. J., and Nix, W. D., Determination of indenter tip geometry and indentation contact area for depth sensing indentation experiments. *J. Mater. Res.* **13**:1300–1306, 1998.

36. Lim, Y. Y., and Chaudhri, Y. Y., The effect of the indenter load on the nanohardness of ductile metals: An experimental study of polycrystalline work-hardened and annealed oxygen-free copper. *Philos. Mag. A.* **79**:2979–3000, 1999.

37. Elmustafa, A. A., and Stone, D. S., Indentation size effect in polycrystalline F.C.C. metals. *Acta Mater.* **50**:3641–3650, 2002.

38. Swadener, J. G., George, E. P., and Pharr, G. M., The correlation of the indentation size effect measured with indenters of various shapes. *J. Mech. Phys. Solids.* **50**:681–694, 2002.

39. Aifantis, E. C., On the microstructural origin of certain inelastic models. *J. Eng. Mater. Technol.* **106**:326–330, 1984.

40. Aifantis, E. C., The physics of plastic deformation. *Int. J. Plasticity.* **3**:211–247, 1987.

41. Arsenlis, A., and Parks, D. M., Crystallographic aspects of geometrically-necessary and statistically-stored dislocation density. *Acta Mater.* **47**:1597–1611, 1999.

42. Voyiadjis, G. Z., and Abu Al-Rub, R. K., *Nonlocal Continuum Damage and Plasticity: Theory and Computation.* World Scientific, Singapore, 2009.

43. Lasry, D., and Belytschko, T., Localization limiters in transient problems. *Int. J. Solids Struct.* **24**:581–597, 1988.

44. Zbib, H. M., and Aifantis, E. C., On the localization and postlocalization behavior of plastic deformation, I, *Res. Mech.* **23**:261–277, 1988.

45. Zbib, H. M., and Aifantis, E. C., On the localization and postlocalization behavior of plastic deformation, II, *Res. Mech.* **23**:279–292, 1988.

46. Zbib, H. M., and Aifantis, E. C., On the localization and postlocalization behavior of plastic deformation, III, *Res. Mech.* **23**:293–305, 1988

47. de Borst, R., and Mühlhaus, H.-B. Gradient-dependent plasticity formulation and algorithmic aspects. *Int. J. Numer. Methods Eng.* **35**:521–539, 1992.

48. de Borst, R., Sluys, L. J., Mühlhaus, H.-B., and Pamin, J., Fundamental issues in finite element analysis of localization of deformation. *Eng. Comput.* **10**:99–121, 1993.

49. Pamin, J., Gradeitn-dependent plasticity in numerical simulation of localization phenomena. Ph.D. diss., Delft University of Technology, Delft, Netherlands, 1994.

50. de Borst, R., and Pamin, J., Some novel developments in finite element procedures for gradient-dependent plasticity. *Int. J. Numer. Methods Eng.* **39**:2477–2505, 1996.

51. Bammann, D. J., Mosher, D., Hughes, D. A., Moody, N. R., and Dawson, P. R., Using spatial gradients to model localization phenomena. Report SAND99-8588. Sandia National Laboratories, Albuquerque, N. M., 1999.

52. Abu Al-Rub, R. K., and Voyiadjis, G. Z., A direct finite element implementation of the gradient plasticity theory. *Int. J. Numer. Meth. Eng.* **63**:603–629, 2005.

53. Eringen, A. C., and Edelen, D. G. B., On nonlocal elasticity. *Int. J. Eng. Sci.* **10**:233–248, 1972.

54. Pijaudier-Cabot, T. G. P., and Bazant, Z. P.,

Nonlocal damage theory. *ASCE J. Eng. Mech.* **113**:1512–1533, 1987.

55. Bazant, Z. P., and Pijaudier-Cobot, G., Nonlocal continuum damage, localization instability and convergence. *J. Appl. Mech.* **55**:287–293, 1988.
56. Fleck, N. A., Muller, G. M., Ashby, M. F., and Hutchinson, J. W., Strain gradient plasticity: Theory and experiment. *Acta Metall. Mater.* **42**:475–487, 1994.
57. Fleck, N. A., and Hutchinson, J. W., A phenomenological theory for strain gradient effects in plasticity. *J. Mech. Phys. Solids.* **41**:1825–1857, 1993.
58. Fleck, N. A., and Hutchinson, J. W., Strain gradient plasticity. *Adv. Appl. Mech.* **33**:295–361, 1997.
59. Fleck, N. A., and Hutchinson, J. W., A reformulation of strain gradient plasticity. *J. Mech. Phys. Solids.* **49**:2245–2271, 2001.
60. Nix, W. D., and Gao, H., Indentation size effects in crystalline materials: A law for strain gradient plasticity. *J. Mech. Phys. Solids.* **46**:411–425, 1998.
61. Gao, H., Huang, Y., Nix, W. D., and Hutchinson, J. W., Mechanism-based strain gradient plasticity—I. Theory. *J. Mech. Phys. Solids.* **47**:1239–1263, 1999.
62. Gao, H., and Huang, Y., Taylor-based nonlocal theory of plasticity. *Int. J. Solids Struct.* **38**:2615–2637, 2001.
63. Hwang, K. C., Jiang, H., Huang, Y., Gao, H., and Hu, N., A finite deformation theory of strain gradient plasticity. *J. Mech. Phys. Solids.* **50**:81–99, 2002.
64. Gurtin, M. E., On the plasticity of single crystals: Free energy, microforces, plastic-strain gradients. *J. Mech. Phys. Solids.* **48**:989–1036, 2000.
65. Gurtin, M. E., A gradient theory of single-crystal viscoplasticity that accounts for geometrically necessary dislocations. *J. Mech. Phys. Solids.* **50**:5–32, 2002.
66. Gurtin, M. E., On a framework for small-deformation viscoplasticity: Free energy, microforces, strain gradients. *Int. J. Plasticity.* **19**:47–90, 2003.
67. Gurtin, M. E., A gradient theory of small-deformation isotropic plasticity that accounts for the Burgers vector and for dissipation due to plastic spin. *J. Mech. Phys. Solids.* **52**:2545–2568, 2004.
68. Gurtin, M. E., and Anand, L., A theory of strain-gradient plasticity for isotropic, plasticity irrotational materials. Part I: Small deformations. *J. Mech. Phys. Solids.* **53**:1624–1649, 2005.
69. Gudmundson, P., A unified treatment of strain gradient plasticity. *J. Mech. Phys. Solids.* **52**:1379–1406, 2004.
70. Abu Al-Rub, R. K., Voyiadjis, G. Z., and Bammann, D. J., A thermodynamic based higher-order gradient theory for size dependent plasticity. *Int. J. Solids Struct.* **44**:2888–2923, 2007.
71. Voyiadjis, G. Z., and Abu Al-Rub, R. K., Nonlocal gradient-dependent thermodynamics for modeling scale dependent plasticity. *Int. J. Multiscale Comput. Eng*. **5**:295–323, 2007.
72. Eringen, A. C., Theory of micropolar elasticity. In *Fracture: An Advanced Treatise*. vol. 2. Liebowitz, H., Ed. Academic Press, New York, 621–729, 1968.
73. Mindlin, R. D., Micro-structure in linear elasticity. *Arch. Ration. Mech. Anal.* **16**:51–78, 1964.
74. Cosserat, E., and Cosserat, F., *Theorie des corp deformables*. Herman, Paris, 1909.
75. Acharya, A., and Bassani, J. L., Lattice incompatibility and a gradient theory of crystal plasticity. *J. Mech. Phys. Solids.* **48**:1565–1595, 2000.
76. Acharya, A., and Beaudoin, A. J., Grain-size effect in viscoplastic polycrystals at moderate strains. *J. Mech. Phys. Solids.* **48**:2213–2230, 2000.
77. Bassani, J. L., Incompatibility and a simple gradient theory of plasticity. *J. Mech. Phys. Solids.* **49**:1983–1996, 2001.
78. Bammann, D. J., A model of crystal plasticity containing a natural length scale. *Mater. Sci. Eng. A.* **309–310**:406–410, 2001.
79. Clayton, J. D., McDowell, D. L., and Bammann, D. J., Modeling dislocations and disclinations with finite micropolar elastoplasticity. *Int. J. Plasticity.* **22**:210–256, 2006.
80. Abu Al-Rub, R. K., and Voyiadjis, G. Z., A

physically based gradient plasticity theory. *Int. J. Plasticity.* **22**:654–684, 2006.

81. Abu Al-Rub, R. K., and Voyiadjis, G. Z., A finite strain plastic-damage model for high velocity impacts using combined viscosity and gradient localization limiters, Part I: Theoretical formulation. *Int. J. Damage Mech.* **15**:293–334, 2006.
82. Mühlhaus, H. B., and Aifantis, E. C., A variational principle for gradient principle. *Int. J. Solids Struct.* **28**:845–857, 1991.
83. Valanis, K. C., A gradient theory of internal variables. *Acta Mech.* **116**:1–14, 1996.
84. Fremond, M., and Nedjar, B., Damage, gradient of damage and principle of virtual power. *Int. J. Solids Struct.* **33**:1083–1103, 1996.
85. Polizzotto, C., and Borino, G., A thermodynamics-based formulation of gradient-dependent plasticity. *Eur. J. Mech. A.* **17**:741–761, 1998.
86. Polizzotto, C., Unified thermodynamic framework for nonlocal/gradient continuum theories. *Eur. J. Mech. A.* **22**:651–668, 2003.
87. Mentzel, A., and Steinmann, P., On the continuum formulation of higher order gradient plasticity for single and polycrystals. *J. Mech. Phys. Solids.* **48**:1777–1796, 2000.
88. Liebe, T., Menzel, A., and Steinmann, P., Theory and numerics of geometrically non-linear gradient plasticity. *Int. J. Eng. Sci.* **41**:1603–1629, 2003.
89. Shizawa, K., and Zbib, H. M., A thermodynamical theory of gradient elastoplasticity with dislocation density tensor. I: Fundamentals. *Int. J. Plasticity.* **15**:899–938, 1999.
90. Svendsen, B., Continuum thermodynamic models for crystal plasticity including the effects of geometrically-necessary dislocations. *J. Mech. Phys. Solids.* **50**:1297–1329, 2002.
91. Voyiadjis, G. Z., Abu Al-Rub, R. K., and Palazotto, A. N., Non-local coupling of viscoplasticity and anisotropic viscodamage for impact problems using the gradient theory. *Arch. Mech.* **55**:39–89, 2003.
92. Voyiadjis, G. Z., Abu Al-Rub, R. K., and Palazotto, A. N., Thermodynamic formulations for non-local coupling of viscoplasticity and anisotropic viscodamage for dynamic localization problems using gradient theory. *Int. J. Plasticity.* **20**:981–1038, 2004.
93. Begley, M. R., and Hutchinson, J. W., The mechanics of size-dependent indentation. *J. Mech. Phys. Solids.* **46**:2049–2068, 1998.
94. Shu, J. Y., and Fleck, N. A., The prediction of a size effect in micro-indentation. *Int. J. Solids Struct.* **35**:1363–1383, 1998.
95. Yuan, H., and Chen, J., Identification of the intrinsic material length in gradient plasticity theory from micro-indentation tests. *Int. J. Solids Struct.* **38**:8171–8187, 2001.
96. Abu Al-Rub, R. K., and Voyiadjis, G. Z., Analytical and experimental determination of the material intrinsic length scale of strain gradient plasticity theory from micro- and nano-indentation experiments. *Int. J. Plasticity.* **20**:1139–1182, 2004.
97. Abu Al-Rub, R. K., and Voyiadjis, G. Z., Determination of the material intrinsic length scale of gradient plasticity theory. *Int. J. Multiscale Comput. Eng.* **3**:50–74, 2004.
98. Abu Al-Rub, R. K., Prediction of micro- and nano indentation size effect from conical or pyramidal indentation. *Mech. Mater.* **39**:787–802, 2007.
99. Voyiadjis, G. Z., and Abu Al-Rub, R. K., Gradient plasticity theory with a variable length scale parameter. *Int. J. Solids Struct.* **42**:3998–4029, 2005.
100. Aifantis, K. E., and Willis, J. R., Scale effects induced by strain-gradient plasticity and interfacial resistance in periodic and randomly heterogeneous media. *Mech. Mater.* **38**:702–716, 2006.
101. Fredriksson, P., and Gudmundson, P., Size-dependent yield strength of thin films. *Int. J. Plasticity.* **21**:1834–1854, 2005.
102. Abu Al-Rub, R. K., Interfacial gradient plasticity governs scale-dependent yield strength and strain hardening rates in micro/nano structured metals. *Int. J. Plasticity.* **24**:1277–1306, 2008.
103. Nye, J. F., Some geometrical relations in dislocated crystals. *Acta Metall.* **1**:153–162, 1953.

104. Voyiadjis, G. Z., Deliktas, B., and Aifantis, E. C., Multiscale analysis of multiple damage mechanisms coupled with inelastic behavior of composite materials. *J. Eng. Mech., ASCE*, **127**:636–645, 2001.
105. Edelen, D. G. B., and Laws, N., On the thermodynamics of systems with nonlocality. *Arch. Ration. Mech. An.* **43**:24–35, 1971.